Time-Resolved Resonance Raman and Density Functional Studies on the Ground State and Short-Lived Intermediates of Tetrabromo-*p*-benzoquinone

Mrinalini Puranik,[†,‡] Jayaraman Chandrasekhar,[‡] Jaap G. Snijders,[§] and Siva Umapathy*[,†,||]

Department of Inorganic and Physical Chemistry, Indian Institute Of Science, Bangalore - 560012, India, Department of Organic Chemistry, Indian Institute Of Science, Bangalore - 560012, India, and Theoretical Chemistry, Materials Science Centre, Nijenborgh 4, 9747 AG Groningen, The Netherlands

Received: February 7, 2001; In Final Form: August 6, 2001

Time-resolved resonance Raman (TR3) and density functional theoretical (DFT) studies on the photogenerated transient intermediates of tetrabromo-*p*-benzoquinone (bromanil) are reported. The lowest triplet excited state, radical anion, and semiquinone radical have been observed. Computed spectra and normal-coordinate analysis have been used to make assignments of the observed bands. The lowest triplet state is computed to be a $\pi-\pi^*$ excited state of ^3B_g symmetry. The effect of electronic excitation on the triplet state structure is found to be more pronounced in bromanil as compared to that in *p*-benzoquinone. The changes in structure in the bromanil radical anion have been explained from the nodal structure of the LUMO of the ground state. The computed structure of the semiquinone radical shows that it is essentially a pentadienyl radical. Consequences of these structural changes on the observed vibrational spectra have been discussed.

1. Introduction

Quinones are involved in a wide range of phenomenon from naturally occurring biological processes to chemical reactions.[1,2] Some of the most interesting reactions of quinones proceed via their photochemically created transient states. Several photoinduced reactions are known, e.g., addition to unsaturated compounds such as olefins, styrenes, acetylenes, and heteroatomic systems.[3−5] Further, because of their extensive use as electron acceptors in charge-transfer salts, they are subjects of several studies for their unique conduction properties.[6] Although the four haloanils and the parent benzoquinone show very different properties, experimental efforts have largely concentrated on the parent quinone[7−19] and its fluorinated and chlorinated analogues.[20−24] Since their electron affinities vary from 1.86 eV for *p*-benzoquinone to 2.95 eV for fluoranil,[25] the effect of different substitutions on the reactivities of these quinones is expected to be significant. Experiments reported in the present paper add toward filling the lacuna of data on the heavier haloanils.

Recent studies on the photoinduced electron-transfer reaction of halogen-substituted *p*-benzoquinones with 2,3-dimethyl-2-butene and 3,4-dimethyl-2-pentene which gave monoallyl ethers have been shown to have product ratios that are highly dependent on the steric nature of the quinones.[26] Several approaches have been used to obtain a better understanding of the structure and spectra of various substituted quinones such as ubiquinones,[27−31] methoxy quinones,[27,32,33] plastoquinones,[34−36] and *p*-benzoquinone[7−19,37−39] and its halogen-substituted analogues,[20−24,40] etc. We have been involved in systematically investigating structures of quinones[24,31,39,41−43] and their short-lived transient states with the specific objective of elucidating their structure−reactivity correlations.

Density functional theoretical (DFT) methods have been used successfully to compute the vibrational spectra not only of the ground state with a good degree of accuracy[22,39,44] but also of radical anions and cations[39,45−48] and triplet states.[39,49,50] In this paper, we have used TR3 and DFT methods in tandem in order to understand the structures and vibrational spectra of bromanil and its transient intermediates and to study the effect of halogen substitution on these short-lived species. In computational studies also, efforts have been concentrated on the prediction of properties of fluorine and chlorine analogues of benzoquinone.[22−24,42] The bromine and iodine analogues have largely been ignored, partly due to the fact that calculations on these systems rapidly become computationally demanding due to their size. It is crucial that the viability of theoretical methods is independently tested for analogues with heavier atoms. Our calculations presented here show that both the ground and the triplet excited state DFT calculations of vibrational spectra can be extended to bromanil successfully. Interestingly, although the ground state spectra have been reported earlier,[40] no calculations have been carried out so far. We present here a complete normal-coordinate analysis of the ground state and transients of bromanil formed on photoexcitation. Relative changes in normal modes have brought out the structural reorganization that occurs in the molecule on electronic excitation, reduction, and substitution. A comparison of the normal modes of bromanil with the parent benzoquinone and other halogen substituted quinones has been presented.

2. Experimental Section

Experimental methods and the procedures used for the TR3 spectroscopy have been described previously.[43] The pump beam is the third harmonic output of a 1064 nm fundamental from a Nd:YAG laser (DCR 11, Spectra Physics). The probe beam is obtained from an optical parametric oscillator (OPO) which is pumped by the third harmonic of 1064 nm output from an

* To whom all correspondence should be addressed. E-mail: umapathy@ipc.iisc.ernet.in. Phone: +91-(0)80-3601234. FAX: +91-(0)80-3600803.
[†] Department of Inorganic and Physical Chemistry, Indian Institute Of Science.
[‡] Department of Organic Chemistry, Indian Institute Of Science.
[§] Theoretical Chemistry, Materials Science Centre.
[||] Swarnajayanti Fellow.

10.1021/jp0104987 CCC: $20.00
Published on Web 10/27/2001

Nd:YAG laser (GCR 250, Spectra Physics). The probe wavelengths of 451 and 512 nm were obtained from the OPO. The pulses had typical energies of 2.5 mJ and were ca. 10 ns in temporal width for both pump and probe lasers. The scattered light was dispersed using a SPEX double monochromator with two 600 grooves/mm gratings. The multichannel detector used was a liquid nitrogen-cooled CCD from Princeton Instruments with 576 × 378 pixels. The spectra have been calibrated using known solvent bands as reference and the spectral resolution has been estimated as 5 cm^{-1}.

Bromanil used was purchased from Aldrich Chemicals and used without further purification. All the solvents as well as bromanil used were of analytical grade. Sample solutions were circulated through a capillary at a rate of about 10 mL per min to avoid possible accumulation of photoproducts. Probe-only spectra were recorded periodically to confirm the absence of photoproducts.

3. Computational Methods

Density functional calculations were performed with the Amsterdam Density Functional (ADF99) package[51] on a cluster of IBM RS 6000/43 P workstations. Calculations for the ground state were carried out using restricted formalism, and those for the triplet excited state used the unrestricted formalism employing open-shell wave functions. The basis set used was TZP (Basis IV in ADF terminology), which is a part of the ADF program.[51] The singlet−triplet gaps were computed using time-dependent density functional theory (TDDFT) calculations as implemented in the response part of the ADF program.[52] Density functional calculations involved the local density approximation of Vosko, Wilk, and Nusair (VWN),[53] the gradient-corrected exchange functional proposed in 1988 by Becke,[54] and the correlation functional of Lee, Yang, and Parr.[55]

4. Results and Discussion

Photochemical reactions of quinones proceed via the triplet excited state which is formed from the photoexcited singlet state by intersystem crossing. The triplet excited state typically undergoes electron transfer from the solvent or hydrogen abstraction or direct decay to the ground state.[56] We have investigated the triplet excited state resonance Raman spectral response with different excitation wavelengths to determine the transient species formed after photoexcitation from the triplet state. Assignments have been made using the results from density functional calculations, using the measured depolarization ratios, and by comparison with other quinones. The structures and vibrational spectra of the transients formed from the triplet excited state viz. the radical anion and the ketyl radical have been examined.

4.1. Time-Resolved Resonance Raman Spectrum of Bromanil in Carbon Tetrachloride and Methanol. Time-resolved resonance Raman spectra of bromanil in carbon tetrachloride are shown in Figure 1. The triplet state was populated using 355 nm excitation of the ground state via intersystem crossing. Resonance Raman spectra were obtained with a probe laser beam tuned at 512 nm, near the absorption maximum of the triplet state.[57] The spectrum shows four bands of varying intensities at 1561, 1395, 1178, and 965 cm^{-1}. The analyses of time-dependent change in intensities indicate (single-exponential decay) that the bands originate from a single intermediate species. The decay rates of all the bands were computed by fitting single exponential and were found to be 0.7 μs, in close agreement with the transient absorption experiments.[58] Since the excitation wavelength used is in resonance with the triplet state, it is expected that only the triplet state modes would be resonance enhanced. Hence, the observed species in carbon tetrachloride is unequivocally identified as the triplet excited state of bromanil. We have measured the depolarization ratios which are close to $^1/_3$ for all the observed bands as expected.[59]

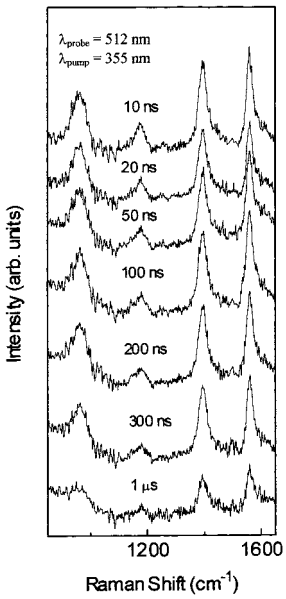

Figure 1. Time-resolved resonance Raman spectra of triplet bromanil in carbon tetrachloride at various time delays between the pump and probe.

The reported absorption spectrum of the potassium salt of bromanil has two bands with maxima at 451 and 331 nm.[60] The time-resolved resonance Raman spectra of bromanil in methanol solution recorded using 451 nm probe excitation wavelength in resonance with the absorption maximum[60] of the radical anion and 355 nm pump excitation are shown in Figure 2. In the probe only spectrum, bands are observed at 1683, 1570, 1546, and 1418 cm^{-1}. The band at 1683 cm^{-1}, was also observed in the probe only spectra recorded at other excitation wavelengths (512 nm) and is identified as a ground state band. The bands observed at 1546 and 1418 cm^{-1} reduce in intensity in the time-resolved spectrum (probe-only spectrum has been subtracted) as the delay time between the pump and probe lasers is increased. The time-resolved resonance Raman spectrum at a pump−probe delay of 10 ns shows a strong band at 1570 cm^{-1} after subtraction of the probe-only signal. Analysis of this slightly asymmetric band by lorenzian fitting suggests that there is a contribution from the band at 1546 cm^{-1} (observed in the probe-only spectrum). Another weak band is observed at later time scales at a shift of 1502 cm^{-1}. Intensity of the band at 1570 cm^{-1} increases up to a delay of 2 μs and then decreases. This temporal behavior implies that presence of two transient species. The bands at 1418 and 1546 cm^{-1} belong to one species, and the band observed at 1570 cm^{-1} has contributions from two species. The spectrum observed at 2 μs is assigned to the radical anion in comparison with our observations of Raman spectra of the chemically prepared radical anion[42] shown in Figure 3a and also with the spectrum reported by Girlando and co-workers.[40] The species giving rise to the bands at 1418 and 1546 and contributing to the intensity of the band at 1570 cm^{-1} is probably of a lower symmetry than C_{2h} since a species with D_{2h} or C_{2h} symmetry is expected to yield only two bands in this region. As quinones are known to undergo electron transfer and hydrogen abstraction reactions in alcohol solvents,[56] comparison with the photochemistry of other substituted quinones suggests that the probable lower symmetry species being

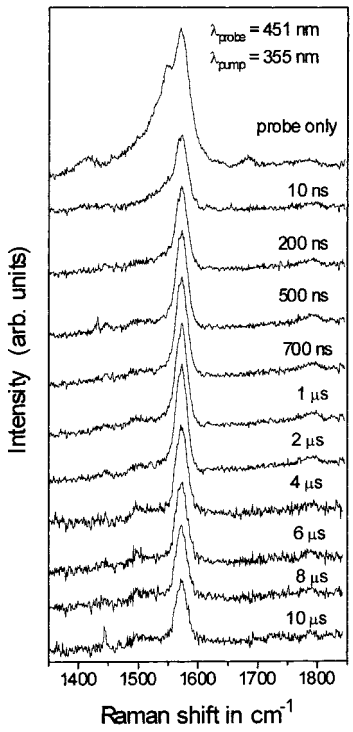

Figure 2. Time-resolved resonance Raman spectra of bromanil in methanol at various time delays between the pump and probe.

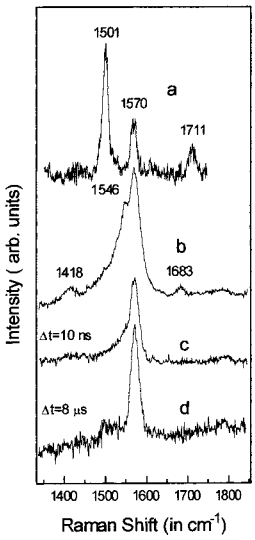

Figure 3. (a) Steady state Raman spectrum of bromanil salt in acetone with excitation at 505 nm; (b) probe-only Raman spectrum of bromanil in methanol with excitation at 451 nm; (c) time-resolved resonance Raman spectrum of bromanil in methanol with $\lambda_{pump} = 355$ nm and $\lambda_{probe} = 451$ nm at a pump−probe time delay of 10 ns; (d) same as panel c, but with a pump−probe time delay of 8 μs.

observed here is the semiquinone radical. The computed spectra (section 4.2) further support this assignment. In this context, akin to bromanil, in benzoquinone and fluoranil the semiquinone radical and the radical anion have been observed (in methanol and water solutions).[8−11,24]

4.2. Structure and Vibrational Assignment. The ground state geometry was optimized using the restricted formalism. For all the other species, unrestricted formalism was used. Throughout the following discussion, we refer to the bonds C_1-C_2 and C_7-C_8, as shown in Figure 4, as C═C irrespective of the actual bond distances. The bonds C_1-C_3, C_3-C_7, C_4-C_2, and C_4-C_8 are equivalent and are labeled C−C. The carbon−

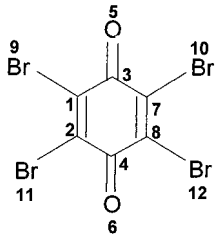

Figure 4. Atom numbering scheme for bromanil.

oxygen bond has been referred to as C═O. Frequencies in the ground, triplet excited state, radical anion, and semiquinone radical were computed at the optimized geometries. We report unscaled frequencies following the recent literature on quinones.[22,23,28,33,39] The computed normal modes were used to determine the potential energy distribution[61−63] using our normal-mode analysis program, NMODES.[39]

The computed HOMO of the ground state is of b_{1g} symmetry. The orbital is of π character with bonding interactions between the carbon atoms of the C═C bond and antibonding interactions between the carbon and bromine atoms of the C−Br bonds. A significant component in the molecular orbital consists of the bromine lone pair that is out of the plane of the molecule. Another occupied orbital of b_{3g} symmetry (HOMO-1) is very close to the HOMO in energy ($\Delta(E_{b_{3g}} - E_{b_{1g}}) = 0.1$ eV). This b_{3g} orbital contains the lone pairs on the oxygen atoms as well as on bromine atoms (in-plane). The corresponding orbital in benzoquinone is concentrated only on the oxygen atoms.[37]

The LUMO is of π^* character and b_{2g} symmetry. It has antibonding interactions between the carbon and the oxygen atoms of the carbonyl groups and the carbon atoms of the C═C bonds. The carbon atoms of the C−C bonds have bonding interaction with each other. As a consequence, the C═C bonds and the C═O bonds are expected to be lengthened, and C−C bonds are expected to be shortened when the LUMO is populated. These characteristics of the molecular orbital are reflected in the calculated triplet state geometries and frequencies (vide infra).

The triplet excited state may be formed by excitation of an electron from either of the orbitals, the HOMO of b_{1g} symmetry or the HOMO-1 of b_{3g} symmetry. Excitation from the b_{1g} orbital to the LUMO (b_{2g}) leads to a triplet excited state of $^3B_{3g}$ symmetry and the excitation from the b_{3g} orbital would yield a triplet state of $^3B_{1g}$ symmetry corresponding to $\pi-\pi^*$ and $n-\pi^*$ triplet states, respectively.

Geometries. Initial geometry optimizations were performed without any symmetry constraints for all the species. The ground state and the radical anion were found to be nearly planar. Following this, the ground state and the radical anion geometries were reoptimized within the constraints of D_{2h} symmetry. The triplet state was found to have a lower symmetry, C_{2h}, with a slight distortion of the bromine atoms and the carbonyl group out of the plane of the C_1, C_2, C_7, and C_8 ring carbon atoms. Optimization of the semiquinone radical was carried out with C_s symmetry with the O−H bond in the plane of the molecule similar to that for the benzoquinone ketyl radical.[37]

Ground State (S_0). Table 1 shows the optimized geometries of the ground and triplet excited states of *p*-benzoquinone and bromanil at the same level of theory. The experimental parameters for *p*-benzoquinone determined from X-ray and electron diffraction experiments by Trotter[64] and Hagen and Hedberg[65] have also been listed for comparison. Since experimental structure of bromanil has not been reported so far, the performance of theory can only be assessed on the basis of the

TABLE 1: Experimental and Calculated Geometries of the Ground and Triplet Excited States of *p*-benzoquinone and Bromanil

	p-benzoquinone (X = H)			bromanil (X = Br)	
	ground state experiment	calculated	triplet state calculated	ground state calculated	triplet state calculated[c]
$R_{(C=C)}$	1.322[a]	1.333	1.345	1.341	1.369
$R_{(C=O)}$	1.222[a]	1.226	1.257	1.212	1.251
$R_{(C-C)}$	1.477[a]	1.469	1.441	1.485	1.440
$R_{(C-X)}$[c]	1.089[b]	1.074	1.071	1.883	1.885
$\alpha_{(C=C-C)}$	121.0[b]	121.3	122.0	121.6	122.2
$\alpha_{(C-C-C)}$	117.8[a]	117.5	116.0	116.9	115.6
$\alpha_{(C=C-X)}$[d]	-	122.7	121.6	123.5	122.8

[a] Ref 64. [b] Ref 65. [c] The triplet state symmetry is C_{2h}. [d] X = H, Br.

data for *p*-benzoquinone. The calculated structural parameters of *p*-benzoquinone agree well with the experimentally determined structure and with the values previously reported in the literature.[39]

The C═C bond distance in ground state of bromanil is calculated to be 1.341 Å, slightly longer than the corresponding distance in *p*-benzoquinone, while the C═O bond is shortened on substitution with bromine by 0.014 Å. The increase in C−C bond length is predicted to be 0.016 Å, which is twice the magnitude of change in C═C bond length. The C−Br bond length is predicted to be 1.883 Å. The angle between the C═C and C−C bonds is increased upon substitution, making the quinone ring elongated along the C_2 axis passing through both the oxygen atoms while maintaining the D_{2h} symmetry. Consequently, angle between the two C−C bonds is smaller. The bromine atoms move away from each other more toward the oxygen atoms than the hydrogen atoms in benzoqinone. This effect may be attributed to large size of bromine atoms compared to hydrogen.

Triplet State (T_1). The two unpaired spins of the triplet state are in molecular orbitals of a_g (1) and b_g (1) symmetry. Therefore, the total symmetry of the triplet state is ^3B_g. Effect of electronic excitation on the geometry of bromanil is largest along the C═O bond with the bond distance increasing from 1.212 Å in the ground state to 1.251 Å (Table 1) in the excited state. Similarly, the C═C bond is also lengthened to 1.369 Å from 1.341 Å. The C−C bonds are shortened to 1.440 Å, which is close the corresponding C−C bond in the triplet state of the parent quinone. The change in C−Br distance is rather negligible when going from the ground to the triplet state. The C═C−C angle increased to 122.8° from 121.6° in the ground state while the C−C−C angle is reduced by 1.3°. The C═C−Br angles suggest that the bromine atoms now move away from the oxygen atoms toward each other. Overall, electronic excitation to the triplet state changes the structure of the ring, making it narrower with the lengths of the C−C bonds reduced. Thus, the ring is distorted considerably in bromanil as compared to the parent quinone along the C_2 axis.

Radical Anion ($BA^{\bullet -}$). Figure 5a shows the optimized geometry of the radical anion of bromanil. The radical anion is formed with the addition of an electron to the LUMO of the ground state. This leads to lengthening of the C═O bond to 1.245 Å and the C═C bond to 1.360 Å. However, the bonding interactions between the $C_1-C_3-C_7$ and $C_2-C_4-C_8$ centers leads to shortening of the C−C bonds from 1.485 Å (in the neutral ground state) to 1.452 Å, and the C−C−C angle is reduced by 3°. The C−Br bond length is enlarged to 1.918 Å. While the overall changes in bond lengths are similar to those observed in the triplet excited state structure, the differences lie along the C−C and C−Br coordinates. The C═C−C angle, which is now 123.2°, is larger than that predicted for the triplet

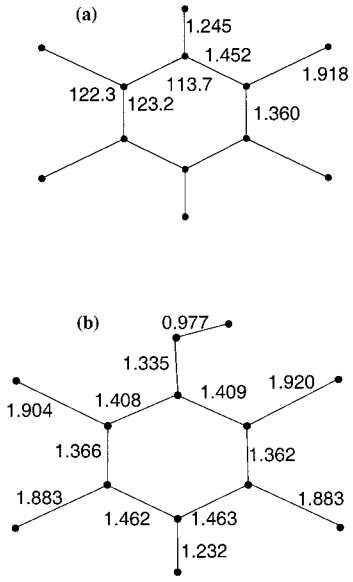

Figure 5. Optimized structures of the bromanil radical anion (a) and semiquinone radical (b).

state, and the C═C−Br angle decreases to 122.3°, similar to the change on triplet excitation. Trends that are observed in the computed structures of radical anions of the parent quinone and its fluorinated and chlorinated analogues are similar.[23] It has been shown earlier that the relative changes in geometries can be qualitatively explained from the nodal structure of the LUMO.[23,42]

Semiquinone Radical ($BQH^{\bullet}$). Figure 5b shows the optimized geometry of the semiquinone radical. Addition of a hydrogen atom to the quinone structure leads to major structural reorganization. The hydrogen atom is bonded to one of the oxygen atoms (O_5), which leads to lengthening of the C_3-O_5 bond by 0.123 Å compared to that in the ground state, whereas the C_4-O_6 bond is lengthened to a much lesser extent. The C_1-C_2 and C_7-C_8 bond lengths are similar to those in the radical anion. The C−C bonds proximal to the site of the addition of hydrogen atom are much shorter (1.408 Å) than the remote C−C bonds (1.462 Å) and also to those observed in the triplet state. The O_5-H_{13} distance is computed to be 0.977 Å (Figure 5b). Changes in the structure of bromanil on abstraction of a hydrogen atom are localized to the part of the molecule proximal to the site of addition. The C−Br bond distances close to the hydrogen atom increase, whereas the remote C−Br bonds are close to their values in the triplet state.

The computed geometrical parameters indicate that the semiquinone is best described as a highly substituted pentadienyl radical. Addition of hydrogen to one of the oxygen atoms of bromanil leaves the distal carbonyl group essentially unperturbed. This has interesting consequences in the vibrational frequencies of the species (vida infra).

Vibrational Frequencies and Normal Modes. Ground State (S_0). Table 2 lists the calculated and experimental frequencies, along with the potential energy distribution for each vibrational mode. From the Raman and IR spectra, in total, 19 fundamental in-plane modes have been observed for the ground state of bromanil[40] of the 30 modes expected (15 *gerade* and 15 *ungerade*). The totally symmetric C═O str. and C═C str. modes are calculated at 1683 and 1577 cm^{-1}, in excellent agreement with the experimental frequencies at 1680 and 1589 cm^{-1}. Both modes are seen to be coupled modes from the PED in Table 2. The experimentally observed mode at 928 cm^{-1} has a computed value of 906 cm^{-1}, underestimated by 22 cm^{-1}. Three low-

TABLE 2: Vibrational Frequencies and Potential Energy Distributions of the In-Plane Normal Modes in the Ground State of Bromanil

sym.	PED(%)	exp[a]	cal
a_g	C═O(80),C−C(11)	1680	1683
	C═C(62), C−C(15), C−Br(8)	1589	1577
	C−C(51), C−Br(48)	928	906
	C−Br(21), C−C(12), δC−C−Br(13), δC═C−C(21), δO═C−C(21)	475	474
	C−Br(72), C−C(22)	214	209
	δC−C−Br(92)		122
b_{3g}	C−C(68), δO═C−C(10), δC═C−C(13)	1235	1176
	C−Br (64), C−C(19), δC═C−C(16)	762	750
	δO═C−C(72), δC−C−Br(12)		694
	δC−C−Br(56), δO═C−C(20), C−Br (12), C−C(12)	282	294
	C−Br (47), C−C(18), δC−C−Br(10), δC═C−C(11)	214	181
b_1u	C═O(79), C−C(14)	1677	1687
	C−C(44), C−Br(32), δC═C−C(24)	1064	1040
	C−C(32), C−Br (28), δC−C−Br(20), δC═C−C(12)	868	863
	C−Br (92)	343	342
	δC−C−Br(58), C−C(25), C−Br (14)	138	134
b_2u	C═C(70), C−Br(12)	1549	1539
	C−C(76), δO═C−C(16)	1216	1169
	C−Br (80), δO═C−C(17)	646	617
	C−Br (48), δO═C−C(28), C−C(16)	343	343
	δBr−C−C(68), C−C(16), C−Br (16)	138	132

[a] Experimental frequencies have been taken from ref 40.

frequency modes of a_g symmetry are computed to be at 474, 209, and 122 cm^{-1}, in close agreement with the observed values of 475, 214, and 127 cm^{-1}. Our calculations predict the band at 474 cm^{-1} as a highly coupled mode with equal contributions from C−Br str., C═C−C bend, and C−C═O bend, whereas Girlando and co-workers[40] have assigned this mode to the C−C−C bend and C−C═O bending. The C−Br str. mode observed here at 209 cm^{-1} is lower than the C−X (X = F, Cl) str. frequencies reported for other quinones.[20,24]

The experimentally observed b_{3g} mode assigned to C−C str. at 1235 cm^{-1} is predicted at 1176 cm^{-1}, a large discrepancy as compared to the typical errors in other calculated frequencies in Table 2. The experimentally observed mode at 762 cm^{-1} that was previously assigned[40] to a combination of C−C−Br bend and C−C═O bend is predicted at 750 cm^{-1}, with major contribution from C−Br stretch (64%).

The infrared active vibrations are predicted with similar accuracy to the Raman active modes. Larger errors are encountered for the higher frequency C═O str. and C−C str. + C−Br str. of b_{1u} symmetry. The remaining lower frequency modes are predicted with a maximum deviation of only 5 cm^{-1}. Of the modes of b_{2u} symmetry listed in Table 2, computed values of are in very good agreement for three lower-frequency modes. For the C═C str. and C−C stretching modes, the errors are slightly larger. It appears from a detailed comparison of the computed and experimental frequencies for the ground state that larger errors are encountered in modes involving the C−C str, C−Br str., and C═C−Br bending coordinates. The overall errors however are less than 30 cm^{-1} for all the modes.

Triplet State (T_1). The observed time-resolved resonance Raman spectrum of the triplet state shows four bands. As in the ground state, two high-frequency modes observed are the C═O and C═C stretching modes. Their order is interchanged in the triplet state with respect to the ordering in the ground state as seen in Table 3. We assign the band observed at 1561 cm^{-1} to the highest frequency C═C stretching coupled to the C═O and C−C stretching predicted at 1525 cm^{-1}. The corresponding mode in the fluorinated[24] and chlorinated[20] analogues are observed at 1667 and 1571 cm^{-1}, thus showing a trend of decreasing C═C stretching frequencies with lowering of the electronegativity of substituents.[20,24] Interestingly, even in the ground state this mode is coupled but with a larger contribution from C═C str. of 62%.

TABLE 3: Computed and Experimental Frequencies and Potential Energy Distributions of the Normal Modes of Triplet Excited State of Bromanil

sym.	PED%	exp	cal
a_g	C═C(35), C−C(27), C═O(20)	1561 (0.35)[a]	1525
	C═O(60), C═C(37)	1395 (0.28)[a]	1311
	C−Br(54), C−C(36)	965 (0.28)[a]	901
	τBr−C−C═O(54), τC−C═O−C(20), τC−C═C−C(26)		728
	C═C(28), δC−C═C(18), δC−C═O(18)		446
	τO═C−C═C(68)		348
	C−Br (81)		214
	δBr−C−C(84)		118
	τBr−C−C═O(68)		84
b_g	C−C(71)		1296
	C−Br(68)		782
	δC−C═O(71), δBr−C−C(25)		678
	τBr−C−C═O(96)		296
	δC−C−Br(40), δC−C═O(24), C−Br(16)		263
	C−Br(46), δC−C−Br(16), δC−C═C(14)		186

[a] Numbers given in parentheses are the measured depolarization ratios.

The band observed at 1395 cm^{-1} is assigned to the C═O stretching mode which is observed at 1621 cm^{-1} in triplet fluoranil[24] and at 1418 cm^{-1} in triplet chloranil,[20] conforming to the same trend as observed in the C═C stretching mode. Calculations predict this mode at 1311 cm^{-1} with a rather large error. This is also a mixed mode with 37% of C═C str. and 60% of C═O str. On the contrary, in the ground state, this mode is almost exclusively a C═O stretching mode. The C═O and C═C stretching modes are important signature modes of the quinones since the relative shifts in these modes in different analogues of benzoquinone reflect changes in the structure due to substitution.[22,23] The band at 965 cm^{-1} is assigned to the computed frequency at 901 cm^{-1}, which corresponds to the C−Br + C−C stretching mode.

In the region around the experimentally observed band at 1178 cm^{-1}, no totally symmetric modes are predicted. One of the possibilities is to assign the mode either to an overtone or a combination band. However, the band has considerable intensity. In the absence of the observation of a corresponding low-frequency fundamental mode of a_g symmetry, the overtone or combination mode is not expected to have such a large intensity. The band may then be assigned to either the fundamental or the overtone or combination band of nontotally symmetric modes. The depolarization ratio (ρ) measured for this band is 0.28. The fundamental of a nontotally symmetric mode is expected to have a ratio of ~0.75, while the overtone/combination of such a mode would be totally symmetric ($\rho \approx 0.33$). Considering that the observed ρ value is close to 0.33, the band at 1178 cm^{-1} may be assigned to an overtone or combination band of a nontotally symmetric mode. However, the fundamental of a nontotally symmetric mode can also be observed due to vibronic coupling and may have a deviation from the expected ρ value.[59] Of the calculated *gerade* wavenumbers, the mode of b_g symmetry closest to the observed band is predicted at 1296 cm^{-1} with a large difference of 118 cm^{-1}. It is therefore not possible to make a definite assignment of this band from the present experiments. Further data of isotropically labeled analogues and spectra at other wavelengths would be required.

Radical anion ($BA^{\bullet -}$). Steady state experimental vibrational spectra of the radical anions of chloranil and bromanil salts have

TABLE 4: Computed and Experimental Frequencies and Potential Energy Distribution of Anion Radical of Bromanil

sym.	PED%	exp[a]	cal
a_g	C═C(22), C−C(28), C═O(33)	1579 (1570)	1558
	C═C(58), C═O(31)	1508 (1502)	1514
	C−C(44), C−Br(52)	955 (942)	922
	δC−C═C(20), C−Br(24), δC−C═O(20)	504 (489)	483
	C−Br (84)	220 (215)	206
	δC−C−Br (92)	...	122
b_{3g}	C−C(71)	1260	1255
	C−Br(66), δC−C═C(20)	722	740
	δC−C═O(70), δC−C−Br(22)	585	683
	δC−C−Br(58), δC−C═O(22)	307	276
	C−Br(76), δC−C═C(17)		185
b_1u	C═O(70), C−C(18)	1518 (1518)	1529
	C−C(56), C−Br(24)	1107 (1098)	1072
	δC−C═C(24), C−Br(44)	880 (871)	853
	C−Br(94)	346	319
	δC−C−Br(61), C−C(20)	...	133
b_2u	C═C(70)	1529	1432
	C−C(78)	...	1090
	C−Br(80), δC−C═O(16)	626	583
	C−Br(53), δC−C═O(31)	346	323
	δC−C−Br(68), C−Br(19)	...	132
	Out-of-Plane Modes		
b_{2g}	τO═C−C−Br(54), τC−C═C−C(25), τC−C═O−C(20)		733
	τO═C−C−C(71)		339
	τO═C−C−Br(66), τO═C−C−C(23)		85
b_{1g}	τO═C−C−Br(100)		281
b_{3u}	τO═C−C−Br(66), τC−C═O−C(26)	687	687
	τO═C−C−C(90)	211	165
	τO═C−C−Br(72), τO═C−C−C(26)		61
a_u	τC−C═O−C(49), τO═C−C−Br(28)		509
	τO═C−C−Br(44), τC−C═C−C(37), τO═C−C−C(23)		38

[a] Experimental frequencies taken from ref 40, numbers in parentheses are band positions in solution.

been observed by Girlando and co-workers.[40] Our time-resolved spectra for the radical anion are in agreement with these data. In Table 4, comparisons of the computed spectra and potential energy distributions with the experimentally observed values are presented. All the frequencies in the solid state are slightly higher than those observed in solution.

The calculated highest frequency a_g mode at 1558 cm^{-1} is observed at 1570 cm^{-1} in solution and assigned to a mixed vibration with nearly equal contributions from the C═C str., the C═O str., and the C−C str. The experimentally observed mode at 1502 cm^{-1} is predicted at 1514 cm^{-1} with a larger C═C stretching character than C═O stretching. This is unlike the cases of other halogen substituted quinones, where C═C stretching frequency is higher than the C═O stretching frequency.[20,39] In the case of the radical anion of the parent benzoquinone,[37] the C═C stretching frequency has been observed at 1620 cm^{-1}, whereas in fluoranil, the two highest frequencies with mixed C═O and C═C stretching characters are observed at 1659 and 1556 cm^{-1}.[24,42] However, in general for the case of bromanil, as discussed earlier for the ground and triplet states, the local mode description becomes an oversimplification. The remaining totally symmetric modes are predicted with smaller errors at 922, 483, and 206 cm^{-1} for the observed bands at 942, 489, and 215 cm^{-1}.

Girlando and co-workers[40] have assigned only the totally symmetric modes from the observed Raman spectra. On the basis of our calculations, we have made tentative assignments for the modes of b_{3g} symmetry, which are summarized in Table 4.

TABLE 5: Computed and Experimental Totally Symmetric Modes and Approximate Assignments for the Semiquinone Radical of Bromanil

sym.	calculated frequencies	approximate assignment
a	3528	O−H str.
	1563 (1574)[a]	C═O str.
	1530 (1546)[a]	C═C str.
	1466	H−C−C bend + C−C str.
	1396 (1418)[a]	C═C str. + C−C str.
	1375	C═O str. + C−C str.

[a] Experimentally observed frequencies in methanol.

The IR active modes are also predicted with a good degree of accuracy. The C═O stretching mode of b_{1u} symmetry is slightly overestimated. The other modes of this symmetry species are all predicted with smaller errors. Five modes of b_{2u} symmetry are predicted, of which three have been observed in the experiment at 1529, 626, and 346 cm^{-1}, corresponding to the computed bands at 1432, 583, and 323 cm^{-1}. Two modes of b_{3u} symmetry observed at 687 and 211 cm^{-1} are computed at 687 and 165 cm^{-1}.

The potential energy distributions of the modes of the radical anion are similar to those predicted for the triplet excited state. The effect of halogen substitution and addition of an electron on the structures of the radical anions is reflected in the modes with dominant contributions from C═C and C═O stretching. For example, in benzoquinone, addition of an electron decreases the observed frequencies from 1665 to 1435 cm^{-1} for the C═O stretch and increases them from 1616 to 1620 cm^{-1} for the C═C stretch.[15,39,66] In bromanil, the ground state frequencies are observed at 1680 cm^{-1} (C═O stretch) and 1589 cm^{-1} (C═C stretch),[40] which shift to 1570 and 1502 cm^{-1} in the radical anion. Hence, the magnitude of change is smaller for the radical anion of bromanil than for benzoquinone. This can be attributed to the inductive effect of the substituent, which lowers the antibonding character of the LUMO, effectively stabilizing the radical anion of the substituted analogue.[42]

Semiquinone Radical (BQH•). The semiquinone radical of bromanil is of C_s symmetry with 23 in-plane modes. The experimentally observed bands are at 1574, 1546, and 1418 cm^{-1} (Table 5). The computed frequencies in this region are at 1563, 1530, 1466, 1396, and 1375 cm^{-1}. The CO stretching mode is predicted at 1563 cm^{-1}; therefore, the band observed at 1574 cm^{-1} is assigned to the CO stretch. The band at 1546 cm^{-1} is assigned to the CC stretch with the predicted value at 1530 cm^{-1}. The remaining band at 1418 cm^{-1} may be assigned to either of the two computed modes at 1375 or 1396 cm^{-1}. The CC and CO stretches at higher frequencies are predicted with errors of 11 and 14 cm^{-1}. Since the same local modes are involved in the present case also, we expect the errors to be of similar magnitude. Hence, we assign the band observed at 1418 cm^{-1} to the CC stretching mode computed at 1396 cm^{-1}.

It is interesting to note that in the semiquinone radical of benzoquinone C═C and C═O bands have been observed at 1613 and 1532, respectively. In fluoranil, the CC stretch of the semiquinone radical is observed at 1645 cm^{-1}, and the CO stretch is observed at 1348 cm^{-1}. Therefore, the ordering of the CC and CO modes is reversed in the predicted spectra for the semiquinone radical of bromanil. The CO stretching frequency is observed at 1680 cm^{-1} in the ground state of bromanil. The mode is shifted to lower frequency in the triplet state (1395 cm^{-1}) and the radical anion (1502 cm^{-1}) due to weakening of the CO bond after population of the antibonding LUMO. In the semiquinone radical, the CO stretch is at 1574 cm^{-1}. Although this is a large reduction compared to the

frequency in the ground state, the effect of protonation is smaller than that introduced by reduction or electronic excitation. This can be understood in terms of the computed structure of the semiquinone radical of bromanil. As pointed out earlier, the distal carbonyl group is not strongly perturbed by the addition of a hydrogen atom. So one of the C═O stretching modes remains at a fairly high frequency in the radical.

5. Summary

The time-resolved resonance Raman spectra of the triplet excited state, radical anion, and semiquinone radical of bromanil have been recorded. Observed vibrational modes have been assigned for all the three transient species by comparison with the ground state frequencies, with spectra computed using density functional calculations, and with other tetrahalogen substituted quinones. Depolarization ratios have been measured for all the observed bands in the triplet excited state. Normal-coordinate analysis has been carried out in order to understand the changes that occur on halogen substitution in the ground and excited states. These data have been used along with the computed frontier molecular orbitals of the ground state to understand the structures of the triplet state, the radical anion, and the semiquinone radical. Our calculations have shown that the participation of the lone pairs on bromine in the frontier molecular orbital is significant.

The effect of halogen substitution is observed to be larger in the triplet excited state than in the ground state. Electronic excitation distorts the molecule to make the ring narrower and the C−C bonds shorter, as well as distorting the molecule out-of-plane to a lower C_{2h} symmetry as compared to the ground state. Vibrational frequencies observed in the triplet state were predicted with larger errors than observed for the ground state. The radical anion geometry is also affected similarly. The changes due to reduction on the structure of bromanil are very similar to the changes due to electronic excitation. However, the C−Br bond lengths show larger changes on reduction than on electronic excitation. These structural changes imply that the radical anion and triplet state of bromanil would be more reactive than the ground state.

The largest structural reorganization is observed in the semiquinone radical. The molecule remains planar with C_s symmetry. Bond lengths and bond angles proximal to the abstracted hydrogen are affected considerably more than the distal ones. The species is essentially a pentadienyl radical, with one carbonyl group left relatively unperturbed.

Both electronic excitation and reduction affect the normal-mode composition. The C═C str. and C═O str. modes are coupled to a greater extent in the triplet state and radical anion than in the ground state. In the ground state, the two high-frequency modes are assigned to the C═O str. and C═C str., whereas in the transient states, both these coordinates have comparable contributions to the two totally symmetric modes.

Acknowledgment. We thank the Department of Science and Technology (DST) and the Council of Scientific and Industrial Research (CSIR) for financial support. M.P thanks Unilever India Inc. and the Dutch Ministry for Culture Education and Science for financial support.

References and Notes

(1) Patai, S., Ed. In *The Chemistry of Quinonoid Compounds*; Wiley: New York, 1974.

(2) Morton, R. A., Ed. In *Biochemistry of Quinones*; Academic Press: New York, 1965.

(3) Girgis, M. M.; Osman, A. H.; Arifien, A. E. *Indian J. Chem*. **1991**, *30A*, 235.

(4) Pla, F. P.; Hall, C. D.; Valero, R.; Pons, M. *J. Chem. Soc., Perkin Trans*. 2 **1994**, 2217.

(5) Shunmugasundaram, A.; Ayyaappan, A.; Thanulingam, T. L. *Indian J. Chem*. **1993**, *32A*, 402.

(6) Fujinawa, T.; Goto, H.; Naito, T.; Inabe, T.; Akutagawa, T.; Nakamura, T. *Bull. Chem. Soc. Jpn*. **1999**, *72*, 21.

(7) Hester, R. E.; Williams, K. P. J. *J. Chem. Soc., Faraday Trans. 2* **1982**, *78*, 573.

(8) Beck, S. M.; Brus, L. E. *J. Am. Chem. Soc.* **1982**, *104*, 4789.

(9) Beck, S. M.; Brus, L. E. *J. Am. Chem. Soc.* **1982**, *104*, 1103.

(10) Rossetti, R.; Beck, S. M.; Brus, L. E. *J. Phys. Chem.* **1983**, *87*, 3058.

(11) Rossetti, R.; Brus, L. E. *J. Am. Chem. Soc.* **1986**, *108*, 4718.

(12) Tripathi, G. N. R.; Schuler, R. H. *J. Phys. Chem.* **1987**, *91*, 5881.

(13) Tripathi, G. N. R. *J. Chem. Phys.* **1981**, *74*, 6044.

(14) Tripathi, G. N. R.; Sun, Q.; Schuler, R. H. *Chem. Phys. Lett*. **1989**, *156*, 51.

(15) Schuler, R. H.; Tripathi, G. N. R.; Prebenda, M. F.; Chipman, D. M. *J. Phys. Chem.* **1983**, *87*, 3101.

(16) Schuler, R. H.; Tripathi, G. N. R.; Prebenda, M. F.; Chipman, D. M. *J. Phys. Chem.* **1983**, *87*, 5357.

(17) Zhao, X.; Imahori, H.; Zhan, C.; Mizutani, Y.; Sakata, Y.; Kitagawa, T. *Chem. Phys. Lett.* **1996**, *262*, 643.

(18) Zhao, X.; Imahori, H.; Zhan, C.; Sakata, Y.; Iwata, S.; Kitagawa, T. *J. Phys. Chem.* **1997**, *101*, 622.

(19) Zhao, X.; Kitagawa, T. *J. Raman Spectrosc.* **1998**, *29*, 773.

(20) Tahara, T.; Hamaguchi, H. *J. Phys. Chem*. **1992**, *96*, 8252.

(21) Tripathi, G. N. R.; Schuler, R. H. *J. Chem. Phys.* **1982**, *76*, 2139.

(22) Boesch, S. E.; Wheeler, R. A. *J. Phys. Chem.* **1995**, *99*, 8125.

(23) Boesch, S. E.; Wheeler, R. A. *J. Phys. Chem.* **1997**, *101*, 8351.

(24) Balakrishnan, G.; Umapathy, S. *Chem. Phys. Lett*. **1997**, *270*, 557. Balakrishnan, G.; Umapathy, S. *J. Chem. Soc., Faraday Trans.* **1997**, *93*, 4125.

(25) Cooper, C. D.; Frey, W. F.; Compton, R. N. *J. Chem. Phys*. **1978**, *69*, 2367.

(26) Kukubo, K.; Masaki, T.; Oshima, T. *Organic Lett.* **2000**, *2*, 1979.

(27) Boullais, C.; Nabedryk, E.; Burie, J.-R.; Nonella, M.; Mioskowski, C.; Breton, *J. Photosynth. Res.* **1998**, *55*, 247.

(28) Nonella, M. *J. Phys. Chem. B* **1998**, *102*, 4217.

(29) Grafton, A. K.; Wheeler, R. A. *J. Phys. Chem. B* **1999**, *103*, 5380.

(30) Boesch, S. E.; Wheeler, R. A. *J. Phys. Chem. A* **1997**, *101*, 5799.

(31) Balakrishnan, G.; Mohandas, P.; Umapathy, S. *Spectrochim. Acta, A* **1997**, *53*, 153.

(32) Burie, J.-R.; Boullais, C.; Nonella, M.; Mioskowski, C.; Nabedryk, E.; Breton, J. *J. Phys. Chem. B* **1997**, *101*, 6607.

(33) Nonella, M.; Brändli, C. *J. Phys. Chem.* **1996**, *100*, 14549.

(34) Razeghifard, M.; Kim, S.; Patzlaff, J. S.; Hutchison, R, S.; Krick, T.; Ayala, I.; Steenhuis, J. J.; Boesch, S. E.; Wheeler, R. A.; Barry, B. A. *J. Phys. Chem. B* **1999**, *103*, 9790.

(35) Grafton, A. K.; Wheeler, R. A. *J. Phys. Chem. A* **1997**, *101*, 7154.

(36) Wise, K. E.; Grafton, A. K.; Wheeler, R. A. *J. Phys. Chem. A* **1997**, *101*, 1160.

(37) Chipman, D. M.; Prebenda, M. F. *J. Phys. Chem.* **1986**, *90*, 5557.

(38) Zhan, C.; Chipman, D. M. *J. Phys. Chem. A* **1998**, *102*, 1230.

(39) Mohandas, P.; Umapathy, S. *J. Phys. Chem. A* **1997**, *101*, 4449.

(40) Girlando, A.; Zanon, I.; Bozio, R.; Pecile, C. *J. Chem. Phys*. **1978**, *68*, 22.

(41) Balakrishnan, G.; Babaei, A.; McQuillan, A. J.; Umapathy, S. *J. Biomol. Struct. Dyn.* **1998**, *16*, 123. Balakrishnan, G.; Umapathy, S. *J. Mol. Struct.* **1999**, *475*, 5.

(42) Puranik, M.; Mohapatra, H.; Balakrishnan, G; Chandrasekhar, J.; Umapathy, S. *Asian J. Phys.* **1998**, *2*, 189.

(43) Balakrishnan, G.; Mohandas, P.; Umapathy, S. *J. Phys. Chem*. **1996**, *100*, 16472.

(44) Biswas, N.; Umapathy, S. *J. Phys. Chem. A* **1997**, *101*, 5555.

(45) Keszthelyi, T.; Wilbrandt, R.; Bally, T. *J. Phys. Chem.* **1996**, *100*, 16843.

(46) Keszthelyi, T.; Wilbrandt, R.; Bally, T.; Roulin, J. L. *J. Phys. Chem.* **1996**, *100*, 16850.

(47) Pan, D.; Shoute, L. C. T.; Phillips, D. L.; *J. Phys. Chem. A* **1999**, *103*, 6851.

(48) Pan, D.; Shoute, L. C. T.; Phillips, D. L.; *J. Phys. Chem. A* **2000**, *104*, 4140.

(49) Weber, P.; Reimers, J. R.; *J. Phys. Chem. A* **1999**, *103*, 9830.

(50) Kamisuki, T.; Hirose, C.; *J. Mol. Struct. (THEOCHEM)* **1998**, *453*, 107.

(51) (a) ADF 1999, Baerends, E. J.; Bérces, A.; Bo, C.; Boerrigter, P. M.; Cavallo, L.; Deng, L.; Dickson, R. M.; Ellis, D. E.; Fan, L.; Fischer, T. H.; Fonseca Guerra, C.; van Gisbergen, S. J. A.; Groeneveld, J. A.; Gritsenko, O. V.; Harris, F. E.; van den Hoek, P.; Jacobsen, H.; van Kessel, G.; Kootstra, F.; van Lenthe, E.; Osinga, V. P.; Philipsen, P. H. T.; Post,

D.; Pye, C. C.; Ravenek, W.; Ros, P.; Schipper, P. R. T.; Schreckenbach, G.; Snijders, J. G.; Sola, M.; Swerhone, D.; te Velde, G.; Vernooijs, P.; Versluis, L.; Visser, O.; van Wezenbeek, E.; Wiesenekker, G.; Wolff, S. K.; Woo, T. K.; Ziegler, T.; (b) Baerends, E. J.; Ellis, D. E.; Ros, P. *Chem. Phys.* **1973**, *2*, 41. (c) Versluis, L.; Ziegler, T.; *J. Chem. Phys.* **1988**, *322*, 88. (d) te Velde, G.; Baerends, E. J. *J Comput. Phys.* **1992**, *99*, 84. (e) Guerra, C. F.; Snijders, J. G.; te Velde, G.; Baerends, E. J. *Theor. Chem. Acc.* **1998**, *99*, 391.

(52) van Gisbergen, S. J. A.; Snijders, J. G.; Baerends, E. J. *Comput. Phys. Commun.* **1999**, *118*, 119.

(53) Vosko, S. H.; Wilk, L.; Nusair, M. *Can. J. Phys*. **1980**, *58*, 1200.

(54) Becke, A. D. *Phys. Rev. A* **1988**, *38*, 3098.

(55) Lee, C.; Yang, W.; Parr, R. G. *Phys. Rev. B* **1988**, *37*, 785.

(56) Bruce, J. M. *Chem. Soc. Q. Rev.* **1967**, *21*, 405.

(57) Hubig, S. M.; Bockman, T. M.; Kochi, J. K. *J. Am. Chem. Soc.* **1997**, *119*, 2926.

(58) Puranik, M.; Balakrishnan, G.; Wilbrandt, R.; Umapathy, S. Manuscript in preparation.

(59) Clark, R. J. H.; Dines, T. J. *Angew. Chem., Int. Ed. Engl.* **1986**, *25*, 131. Hamaguchi, H. In *Advances in Infrared and Raman Spectroscopy*; Clark, R. J. H., Hester, R. E., Eds.; Wiley: Chichester, 1985; Vol. 12, p 273.

(60) Iida, Y *Bull. Chem. Soc. Jpn.* **1970**, *43*, 2772.

(61) Gans, P. Force Constant Calculationas: The State of the Art. In *Advances in Infrared and Raman Spectroscopy*; Clark, R. J. H., Hester, R. E. Eds.; Heyden: London, 1977; p 87.

(62) Needham, C. D.; Overend, J. *Spectrochim. Acta* **1966**, *22*, 1383.

(63) Christopher, R. E.; Gans, P. *J. Chem. Soc., Dalton Trans.* **1975**, 153.

(64) Trotter, J. *Acta Crystallogr*. **1960**, *13*, 86.

(65) Hagen, K.; Hedberg, K. *J. Chem. Phys.* **1973**, *59*, 158.

(66) Becker, E. D. *J. Phys. Chem.* **1991**, *95*, 2818.